JCB Article

Identification of an organelle-specific myosin V receptor

Kuniko Ishikawa, Natalie L. Catlett, Jennifer L. Novak, Fusheng Tang, Johnathan J. Nau, and Lois S. Weisman

Department of Biochemistry, The University of Iowa, Iowa City, IA 52242

Class V myosins are widely distributed among diverse organisms and move cargo along actin filaments. Some myosin Vs move multiple types of cargo, where the timing of movement and the destinations of selected cargoes are unique. Here, we report the discovery of an organelle-specific myosin V receptor. Vac17p, a novel protein, is a component of the vacuole-specific receptor for Myo2p, a *Saccharomyces cerevisiae* myosin V. Vac17p interacts with the Myo2p cargo-binding domain, but not with vacuole inheritance-defective *myo2* mutants that have single amino acid changes within this region. Moreover, a region of the Myo2p tail required specifically for secretory vesicle transport is neither required for vacuole inheritance nor for Vac17p–Myo2p interactions. Vac17p is localized on the vacuole membrane, and vacuole-associated Myo2p increases in proportion with an increase in Vac17p. Furthermore, Vac17p is not required for movement of other cargo moved by Myo2p. These findings demonstrate that Vac17p is a component of a vacuole-specific receptor for Myo2p. Organelle-specific receptors such as Vac17p provide a mechanism whereby a single type of myosin V can move diverse cargoes to distinct destinations at different times.

Introduction

Myo2p moves secretory vesicles (Govindan et al., 1995; Schott et al., 1999), the Golgi (Rossanese et al., 2001), the vacuole (Hill et al., 1996; Catlett and Weisman, 1998; Catlett et al., 2000), and the mitotic spindle (Beach et al., 2000; Yin et al., 2000). The time of movement and the final destinations of these cargoes, while overlapping, are not identical. At the onset of the cell cycle, the organelles are targeted to the presumptive bud site. However, at cytokinesis, secretory vesicles are targeted to the mother-bud neck, whereas vacuoles are localized at the central regions within both the mother and bud cells. Thus, the attachment and/or activation of Myo2p on distinct organelles must be differentially regulated.

The globular tail of myosin V plays an important role in its attachment to cargo. Overexpression of the globular tail of myosin Va causes a defect in melanosome movement (Wu et al., 2002a); likewise, overexpression of the globular tail of Myo2p disrupts secretory vesicle targeting and causes cell death (Reck-Peterson et al., 1999; Schott et al., 1999). In both cases, overexpression of this domain is thought to compete with endogenous myosin V and displace it from cargo. Additionally, cell cycle–specific phosphorylation of the myosin Va globular tail releases it from membranes (Karcher et al., 2001), suggesting that post-translational modification of the tail may be important for its attachment to cargo.

The globular tail of Myo2p contains at least two distinct cargo-binding domains, one specific for vacuole movement (Catlett and Weisman, 1998; Catlett et al., 2000), the other specific for secretory vesicles (Schott et al., 1999; Catlett et al., 2000). The vacuole-specific region was defined by seven point mutations affecting one of five amino acids between residues 1248–1307 of the Myo2p globular tail domain. The secretory vesicle binding domain was identified via sequence analysis of a set of *myo2*^{ts} mutants (Schott et al., 1999), and by identification of *myo2-Δ1459–1491*, a mutant specifically defective in secretory vesicle movement (Catlett, 2000). Overexpression of the Myo2p globular tail missing the secretory vesicle–specific region disrupts vacuole inheritance, but does not affect secretory vesicle targeting. Conversely, mutations in the vacuole-binding domain cause defects in vacuole movement, but do not affect other Myo2p-related functions such as secretion. Given that specific regions of the globular tail are required for different functions of Myo2p, the existence of cargo-specific receptors for Myo2p was predicted. Here, we describe Vac17p, a novel protein that is a key component of the vacuole-specific Myo2p receptor.

N.L. Catlett and K. Ishikawa contributed equally to this paper.

Address correspondence to Lois S. Weisman, Dept. of Biochemistry, The University of Iowa, Iowa City, IA 52242. Tel.: (319) 335-8581. Fax: (319) 335-9570. E-mail: lois-weisman@uiowa.edu

N.L. Catlett's present address is Torrey Mesa Research Institute, Syngenta Research and Technology, 3115 Merryfield Row #100, San Diego, CA 92121.

Key words: membrane transport; Myo2p; Vac17p; yeast; vacuole

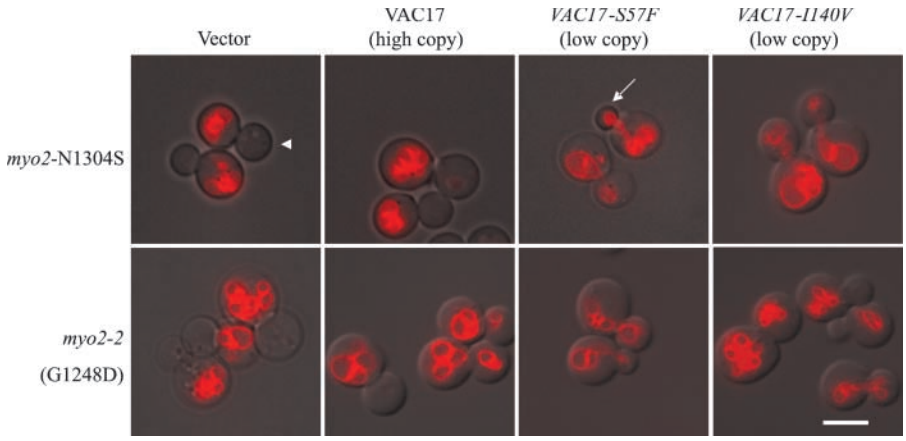

Figure 1. **Vac17p was obtained in two screens designed to identify the vacuole-specific Myo2p receptor.** The vacuole inheritance defect in *myo2–2* was suppressed by high copy *VAC17*. The vacuole inheritance defects in *myo2-N1304S* and *myo2–2 (myo2-G1248D)* were suppressed by the presence of either *VAC17-S57F* or *VAC17-I140V*. Strains were labeled for 1 h with the vacuole-specific fluorophore FM4–64, and were chased in fresh media for 4 h. The arrow and arrowhead indicate an example of a bud with and without an inherited vacuole, respectively. Bar, 5 μm.

Results

To identify the vacuole-specific myosin V receptor, we designed two genetic screens. First, we sought multicopy suppressors of *myo2–2* (*myo2-G1248D*), guessing that the impaired association of myo2–2p with vacuole (Catlett and Weisman, 1998) might be overcome by increasing levels of the receptor or of other proteins required for Myo2p-mediated vacuole movement. The second screen sought mutations in genes other than *MYO2* that would restore vacuole inheritance in a vacuole-specific *myo2* point mutant, *myo2-N1304S*; and was based on the hypothesis that a weakened protein–protein interaction caused by *myo2-N1304S* might be restored by a compensatory mutation in the binding partner. Furthermore, the location of the point mutation in the binding partner might reveal additional information indicating which region of the receptor contacts the globular tail of Myo2p. We obtained *VAC17* as a multicopy suppressor of *myo2–2* and the point mutant *VAC17-S57F* as a genomic mutation suppressing *myo2-N1304S*. *VAC17* had also been identified as the corresponding wild-type gene of the vacuole inheritance mutant *vac17* (Tang et al., 2003) and as encoding a protein interacting with the vacuolar membrane protein Vac8p (Tang et al., 2003).

Surprisingly, *VAC17-S57F* suppressed the vacuole inheritance defect of all the vacuole-specific *myo2* tail mutants (Fig. 1 and Table I). These findings prompted us to perform a directed screen for other mutations in *VAC17* that could suppress the vacuole inheritance defect of *myo2-N1304S*. We identified a second amino acid substitution (*VAC17-I140V*) that showed allele specificity, as it only suppressed the vacuole inheritance defects of *myo2–2*, *myo2-N1304S,* and *myo2-N1307D* (Fig. 1 and Table I).

The above genetic interactions and the requirement for Vac17p in vacuole inheritance (Fig. 2; Tang et al., 2003) suggest that Vac17p plays a key role in Myo2p-mediated vacuole movement. Moreover, the *vac17*Δ strain displays no growth defects, suggesting that Vac17p is not required for secretory vesicle transport (Tang et al., 2003). Next, we tested whether Vac17p is required for movement of other cargo carried by Myo2p. Inheritance of the late Golgi and peroxisomes requires Myo2p, as defects in the inheritance of both organelles are observed in the *myo2–66* mutant (Fig. 2; Hoepfner et al., 2001; Rossanese et al., 2001). In contrast, inheritance of these organelles is normal in the *vac17*Δ mutant (Fig. 2). Myo2p also functions in nuclear spindle orientation (Beach et al., 2000; Yin et al., 2000). Consistent with these observations, *myo2–2* cells are defective in nuclear migration, as demonstrated by a significant increase in binucleate cells (Fig. 2 C, column 7). However, nuclear partitioning is normal in *vac17*Δ. We also investigated mitochondrial inheritance in

Table I. **VAC17-S57F, VAC17-I140V, and high copy VAC17 suppress the vacuole inheritance defects of selected vacuole-specific myo2 tail mutants**

	Suppressor		Wild-type VAC17		
	VAC17-S57F	VAC17-I140V	High copy	Low copy	Vector
myo2	%	%	%	%	%
WT	97	98	95	97	98
G1248D	63	62	30	16	11
D1297N	56	20	12	12	8
D1297G	63	15	14	9	11
L1301P	50	24	11	10	10
N1304D	59	18	ND	8	8
N1304S	64	50	18	13	11
N1307D	56	47	ND	12	10

Vacuole inheritance was measured by counting the percentage of cells with an inherited vacuole in the bud. Control strains with vector alone, low copy (pRS416), or high copy (pRS426) gave similar values, but only pRS416 is shown. Each strain was counted at least three times, with a minimum total of 200 cells scored. ND, not determined.

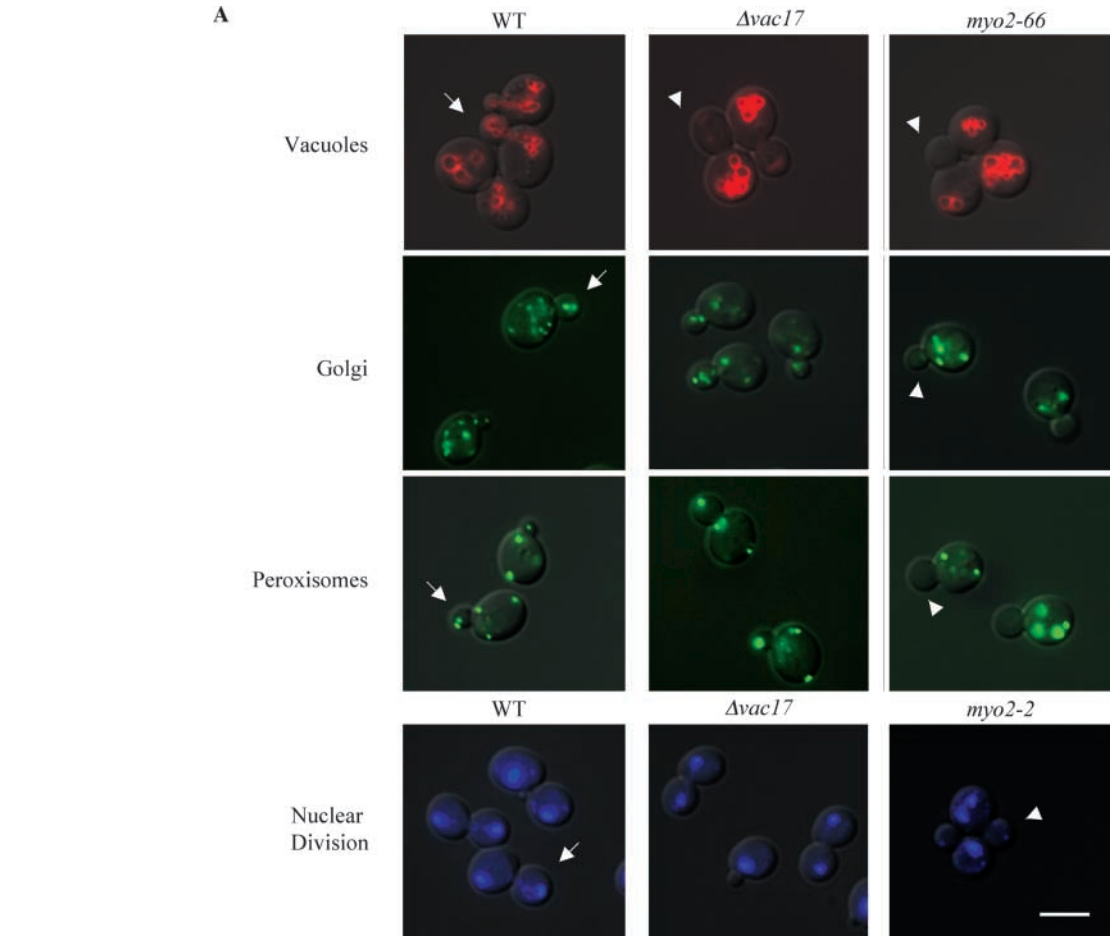

Figure 2. **Vac17p is required for inheritance of vacuoles, but not for inheritance of Golgi, peroxisomes, mitochondria, or nuclei.** (A) Fluorescence micrographs of the indicated organelles and strains. Examples of buds with (arrow) and without (arrowhead) the relevant organelles are indicated. Vacuoles were labeled for 1 h with FM4–64 and chased in fresh media for 2 h. Golgi were visualized with Sec7p-GFP. Peroxisomes were visualized with GFP fused to the peroxisome-targeting signal PTS1 (GFP-PTS1). Nuclei were labeled using DAPI. Images of Sec7p-GFP– and GFP-PTS1–labeled cells were obtained by merging five Z-axis planes spaced by 0.75 μM. *myo2–66* is defective in vacuole, Golgi, and peroxisome inheritance, *myo2–2* is defective in nuclear segregation. Bar, 5 μm. (B) Quantification of vacuole, Golgi, and peroxisome inheritance. Vacuole inheritance is reported as percentage of cells with an inherited vacuole in the bud. Golgi inheritance was assessed in cells with buds less than one third the size of the mother. Peroxisome inheritance was assessed in cells with buds less than half the size of the mother. For each strain, cells were scored from at least two independent experiments. (C) Quantification of nuclear segregation. Each strain was counted in four independent experiments. Cell types are reported as percentage of total cells.

*vac17*Δ cells and observed no defect (unpublished data). Thus, Vac17p appears to be solely required for vacuole movement.

As predicted for a receptor for Myo2p, Vac17p interacts with the Myo2p globular tail (Fig. 3 A). Notably, although the interaction between full-length Vac17p (1–425) and the Myo2p globular tail (1113–1574) was weak, removal of the secretory vesicle–binding domain from the Myo2p tail (Δ1459–1491) consistently increased Vac17p–Myo2p interactions (Fig. 3 A). Note that these fusion proteins were expressed to similar levels (Fig. 3 B). This suggests that Myo2p attachment to Vac17p may be regulated to ensure that only one type of cargo binds at any given moment. Likewise, compared with

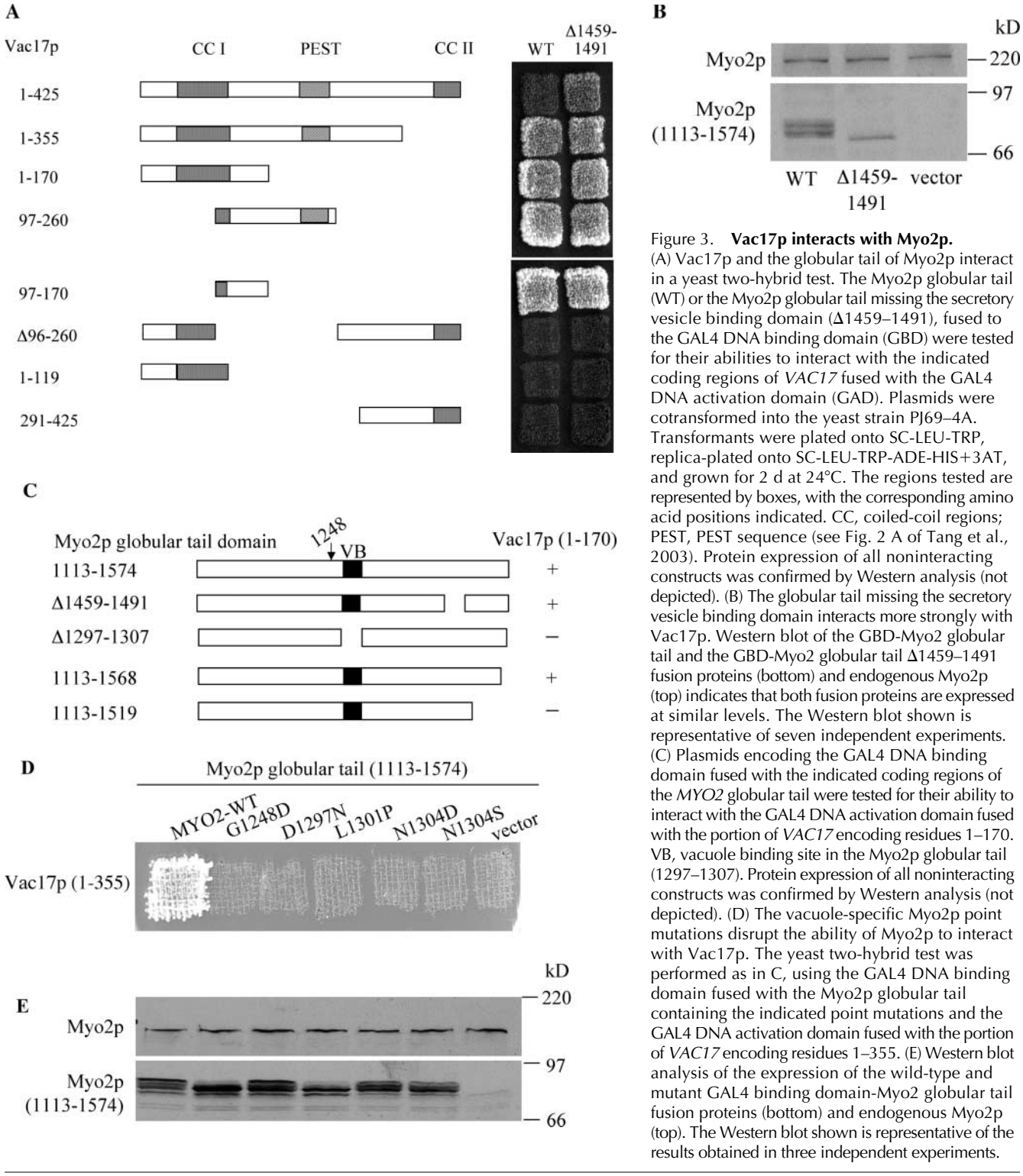

Figure 3. **Vac17p interacts with Myo2p.** (A) Vac17p and the globular tail of Myo2p interact in a yeast two-hybrid test. The Myo2p globular tail (WT) or the Myo2p globular tail missing the secretory vesicle binding domain (Δ1459–1491), fused to the GAL4 DNA binding domain (GBD) were tested for their abilities to interact with the indicated coding regions of *VAC17* fused with the GAL4 DNA activation domain (GAD). Plasmids were cotransformed into the yeast strain PJ69–4A. Transformants were plated onto SC-LEU-TRP, replica-plated onto SC-LEU-TRP-ADE-HIS+3AT, and grown for 2 d at 24°C. The regions tested are represented by boxes, with the corresponding amino acid positions indicated. CC, coiled-coil regions; PEST, PEST sequence (see Fig. 2 A of Tang et al., 2003). Protein expression of all noninteracting constructs was confirmed by Western analysis (not depicted). (B) The globular tail missing the secretory vesicle binding domain interacts more strongly with Vac17p. Western blot of the GBD-Myo2 globular tail and the GBD-Myo2 globular tail Δ1459–1491 fusion proteins (bottom) and endogenous Myo2p (top) indicates that both fusion proteins are expressed at similar levels. The Western blot shown is representative of seven independent experiments. (C) Plasmids encoding the GAL4 DNA binding domain fused with the indicated coding regions of the *MYO2* globular tail were tested for their ability to interact with the GAL4 DNA activation domain fused with the portion of *VAC17* encoding residues 1–170. VB, vacuole binding site in the Myo2p globular tail (1297–1307). Protein expression of all noninteracting constructs was confirmed by Western analysis (not depicted). (D) The vacuole-specific Myo2p point mutations disrupt the ability of Myo2p to interact with Vac17p. The yeast two-hybrid test was performed as in C, using the GAL4 DNA binding domain fused with the Myo2p globular tail containing the indicated point mutations and the GAL4 DNA activation domain fused with the portion of *VAC17* encoding residues 1–355. (E) Western blot analysis of the expression of the wild-type and mutant GAL4 binding domain-Myo2 globular tail fusion proteins (bottom) and endogenous Myo2p (top). The Western blot shown is representative of the results obtained in three independent experiments.

full-length Vac17p, specific truncations of Vac17p increased Vac17p–Myo2p interactions. This behavior suggests that regions outside of the Myo2p binding domain of Vac17p function in the negative regulation of Vac17p–Myo2p interactions.

Analysis of the Vac17p truncations showed that the Myo2p binding domain on Vac17p lies between residues 97–170. In further support of the above two-hybrid analysis, deletion of this region (*vac17-Δ109–190*) abrogates vacuole inheritance (Tang et al., 2003).

Deletion analysis of Myo2p showed that removal of residues 1297–1307 abolished Vac17p–Myo2p interactions (Fig. 3 C). However, this short sequence is not sufficient for Vac17p binding, as the shortest segment of the tail that interacts with Vac17p (residues 1113–1568) encompasses nearly the entire globular tail (Fig. 3 C).

To determine if the vacuole inheritance defects seen in the *myo2* tail mutants result from poor interaction of the mutant Myo2p with Vac17p, we examined interaction of Vac17p

(1–355) with myo2p tail fusions of five representative mutants (*myo2–2*/G1248D, D1297N, L1301P, N1304D, and N1304S). None of these constructs interacts significantly with Vac17p (Fig. 3 D). Western blot analysis indicates that all of these mutant Myo2p fusion proteins were expressed to a similar degree as wild type (Fig. 3 E). Together with the requirement of Vac17p in vacuole inheritance, these observations suggest that the interaction of Vac17p and Myo2p is normally required for vacuole movement.

We further analyzed the relationship between Vac17p–Myo2p interactions and vacuole inheritance by testing the interaction of additional *myo2* mutants with Vac17p. As part of a separate paper (Catlett, N.L., unpublished data), we obtained a collection of intragenic suppressors of the *myo2–2* (G1248D) vacuole inheritance defect via random PCR mutagenesis. Eight of these suppressors restore vacuole inheritance to >80% when present as the sole copy of *MYO2*. Each suppressor, except the pseudorevertant G1248N, contains both G1248D and a second point mutation. We constructed myo2 tail DNA binding-domain fusions of these suppressors and found that all eight simultaneously restored vacuole inheritance and Vac17p–Myo2p interactions. This finding demonstrates that the vacuole inheritance defect in *myo2–2* is directly related to a loss of Vac17p–Myo2p interactions.

Analysis of *VAC17-I140V* also strongly supports the hypothesis that Vac17p–Myo2p interactions are required for vacuole inheritance. The I140V mutation is located in the Myo2p binding site. *VAC17-I140V* restored vacuole inheritance in *myo2-N1304S* from ~10 to 50% (Table I). Moreover, it showed allele specificity, restoring vacuole inheritance in *myo2–2* (G1248D), N1304S, and N1307D, but not in other vacuole-specific *myo2* point mutants (Table I). Next, we tested whether *VAC17-I140V*, in addition to restoring vacuole inheritance, restored interaction with *myo2–2* and *myo2-N1304S* (Fig. 4 D). A *VAC17-I140V* two-hybrid construct (97–260) restored interaction with both *myo2–2* and *myo2-N1304S.* A longer fusion, *VAC17-I140V* (1–260) also interacted with the globular tail domain of *myo2–2*. The suppression of *myo2–2* by I140V is not due to overexpression of Vac17p because its levels are similar to the wild-type protein (unpublished data). Thus, *VAC17-I140V* suppresses selected vacuole-specific *myo2* mutants by increasing the affinity of Vac17p for Myo2p through the original interaction site.

Characterization of *VAC17-I140V* strongly suggests that Vac17p binds to Myo2p directly. That *VAC17-I140V* causes an allele-specific, extragenic restoration of vacuole inheritance in the *myo2–2* mutant, concomitant with the restoration of Vac17p–Myo2p interactions, is best explained by the re-establishment of a direct interaction between the two proteins. In further support of a direct interaction between Vac17p and Myo2p, we found that Myo2p coimmunoprecipitates with Vac17p (Tang et al., 2003).

Although Vac17p interacts with Myo2p and also Vac8p (Tang et al., 2003), our analysis of *VAC17-S57F* suggested that Vac17p also interacts with yet another molecule to regulate Myo2p attachment to the vacuole. The molecule predicted by the behavior of *VAC17-S57F* is unlikely to be Vac8p because the Vac17p-S57F mutation maps outside of the Vac8p binding region (Tang et al., 2003). Moreover, *VAC17* and *VAC17-S57F* interact with *VAC8* to the same extent (unpublished data).

Evidence that Vac17p interacts with at least one additional molecule includes the following: First, *VAC17-S57F* showed no allele specificity, suppressing all of the vacuole-specific *myo2* point mutants to a similar degree (Fig. 2 B). Second, although *VAC17-S57F* interacted with wild-type Myo2p, it did not restore interactions with the vacuole-specific Myo2p point mutants (Fig. 4 D). Furthermore, the S57F mutation maps outside of the Myo2p binding region of Vac17p (Fig. 4 C). Finally, this region of Vac17p is not essential for vacuole inheritance; removal of residues 1–97 from Vac17p reduces vacuole inheritance by only 30% (unpublished data). The most likely explanation for these data is that Vac17p-S57F indirectly restores Vac17p–Myo2p interactions, suggesting that at least one other protein is involved in Myo2p binding to Vac17p. This protein could be part of the receptor complex and could work with Vac17p to promote Myo2p interaction with vacuole. Alternatively, the protein might negatively regulate Vac17p–Myo2p interactions, but not Vac17p-S57F–Myo2p interactions. The suppression by *VAC17-S57F* is not due to elevated Vac17p levels; the cellular concentration of Vac17p-S57F is the same as the wild-type protein (unpublished data). Also, it is unlikely that the S57F mutation now allows Vac17p to interact with Myo2p at a site distinct from the globular tail. Using the yeast two-hybrid test, we found no interaction between Vac17p-S57F and the Myo2p tail containing both the globular domain and the coiled-coil region or the coiled-coil region alone (unpublished data).

By definition, the vacuole-specific receptor for Myo2p would recruit the motor to the vacuole. Thus, using double-labeled immunofluorescence microscopy, we tested whether Vac17p is required for the association of Myo2p with vacuoles. In addition, we used Western analysis to measure the level of Myo2p on isolated vacuoles. For these experiments, WT, *vac17*Δ, and *VAC17-*Δ*PEST* cells were compared. The removal of the PEST sequence stabilizes Vac17p, increasing the levels of Vac17p on the vacuole (Tang et al., 2003). This mutant, expressed from a low copy plasmid, was used instead of high copy *VAC17* because the number of multicopy plasmids present varies widely from cell to cell. Like overexpression of Vac17p from a multicopy plasmid, *VAC17-*Δ*PEST* increases vacuole inheritance in *myo2–2* from 11 to 37% (n = 187), but does not affect vacuole inheritance in *myo2-N1304S* (n = 232).

In wild-type cells, Myo2p concentrates at sites of polarized growth and is also present as small cytoplasmic spots, with a subset of spots colocalizing with the vacuolar membrane (Hill et al., 1996 and Fig. 5 A). Thus, the low levels of vacuolar Myo2p seen by immunofluorescence microscopy are insufficient to determine whether less Myo2p is present on vacuoles in *vac17*Δ cells. However, increasing Vac17p levels with the Vac17p-stabilizing mutant *VAC17-*Δ*PEST* (Tang et al., 2003) dramatically increased the levels of Myo2p on the vacuole (Fig. 5 C). Consistent with the immunofluorescence microscopy images, when compared with wild type, significantly higher levels of Myo2p copurified with *VAC17-*Δ*PEST* mutant vacuoles. Moreover, levels of Myo2p on *vac17*Δ vacuoles were significantly lower (Fig. 5

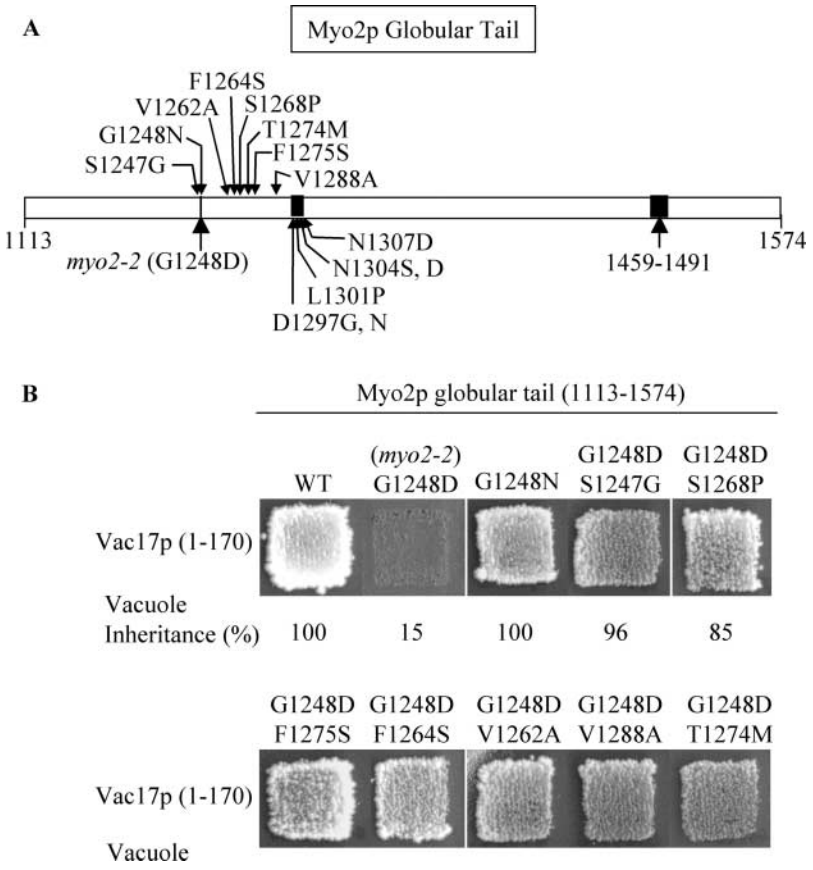

Figure 4. **All intragenic *myo2–2* suppressors restore both vacuole inheritance and Vac17p–Myo2p interactions.** Likewise, *VAC17-I140V* suppresses the vacuole-specific Myo2p tail mutants *myo2–2* and *myo2-N1304S,* and interacts with the Myo2p globular tail containing either of these point mutations. (A) Schematic of the Myo2p globular tail. Arrows above the schematic indicate the amino acid changes that suppress the vacuole inheritance defect of *myo2–2* (G1248D), whereas arrows below the schematic indicate the vacuole-specific point mutations at residues 1248, 1297, 1301, 1304, and 1307, and the secretory vesicle–specific region (1459–1491). (B) The yeast two-hybrid test was used to assess the ability of the Myo2p globular tail containing the *myo2–2* intragenic suppressor point mutations to bind to Vac17p (1–170). Vacuole inheritance was assessed by scoring the percentage of cells with buds containing an inherited vacuole. Each of the *myo2–2* intragenic suppressors was tested as the sole copy of the *MYO2* gene. A minimum total of 180 cells were counted from three independent experiments. (C) Schematic of Vac17p showing the location of the *VAC17* mutations S57F and I140V. CCI and CCII indicate predicted coiled-coil regions. PEST indicates a predicted protein degradation signal. Further analysis of the Vac17p sequence is described in Tang et al. (2003). (D) The yeast two-hybrid test was used to assess the ability of *VAC17-I140V* and *VAC17-S57F* to interact with the globular tail of *myo2–2* and *myo2-N1304S*. The region of *VAC17* initially

E). The above data strongly suggests that Vac17p is required for normal Myo2p association with the vacuole.

We included *myo2–2* mutant vacuoles as we had previously observed that myo2–2p was severely defective in its association with the vacuole (Catlett and Weisman, 1998). However, in this work, the defect in myo2–2p association with the vacuole appears less severe. The vacuole isolation conditions for the current work included additional protease inhibitors that were not used in the previous work. Vacuoles isolated from *vac17–1*, or *vac8*Δ cells without the addition of these extra protease inhibitors showed no significant difference in Myo2p levels as compared with wild-type vacuoles (Catlett, N.L., unpublished data).

Discussion

Several lines of evidence suggest that Vac17p is a key component of the vacuole-specific Myo2p receptor. Vac17p is required for vacuole inheritance, and residues 96–170 of Vac17p bind directly to the globular tail of Myo2p. Furthermore, Vac17p is localized on the vacuole membrane (Tang et al., 2003), and it is required for Myo2p association with the vacuole. Moreover, Vac17p resides on the vacuole membrane through interaction of its COOH terminus with the myristylated and palmitoylated vacuolar membrane protein Vac8p (Tang et al., 2003). We propose that Myo2p associates with the vacuole via direct interaction with Vac17p, which in turn binds directly to Vac8p (Fig. 5 F).

The molecular basis of Myo2p attachment to the vacuole shares similarities to what is currently known about myosin Va attachment to melanosomes. Melanophilin, a recently discovered rab effector, is a component of the melanosome-specific myosin Va receptor (Fukuda and Kuroda, 2002; Hume et al., 2002; Nagashima et al., 2002; Provance et al., 2002; Wu et al., 2002b). Melanophilin binds directly to myosin V, and interacts with melanosomes via interaction with Rab27a. Thus, both Vac17p and melanophilin bind directly to myosin V and attach to their respective membranes via interaction with an acylated protein.

Despite these similarities, there are several differences between attachment of myosin Va to melanosomes and Myo2p attachment to vacuoles. Melanophilin and Vac17p do not share any sequence similarity. Moreover, no obvious melanophilin homologues were found in the yeast genome database. Similarly, no Vac17p homologues were found in higher eukaryotes. In addition, Rab27a and Vac8p are not related proteins. Vac8p is not a small GTPase; rather, it likely plays its role via interaction with binding partners. It appears that Vac8p brings specific protein complexes to distinct regions of the vacuole (Wang et al., 2001). Moreover, although both Vac8p and Rab27a are acylated, Rab27a is geranylgeranylated at its COOH terminus, and Vac8p is myristylated and multiply-palmitoylated at is NH_2 terminus. These diverse types of modifications are likely to serve distinct functions (Melkonian et al., 1999; Zacharias et al., 2002).

It is possible that the differences in these receptors arise because their respective membranes are found in distant organisms or because the melanosome is a specialized lysosomal-like organelle, whereas the yeast vacuole/lysosome serves more generalized functions.

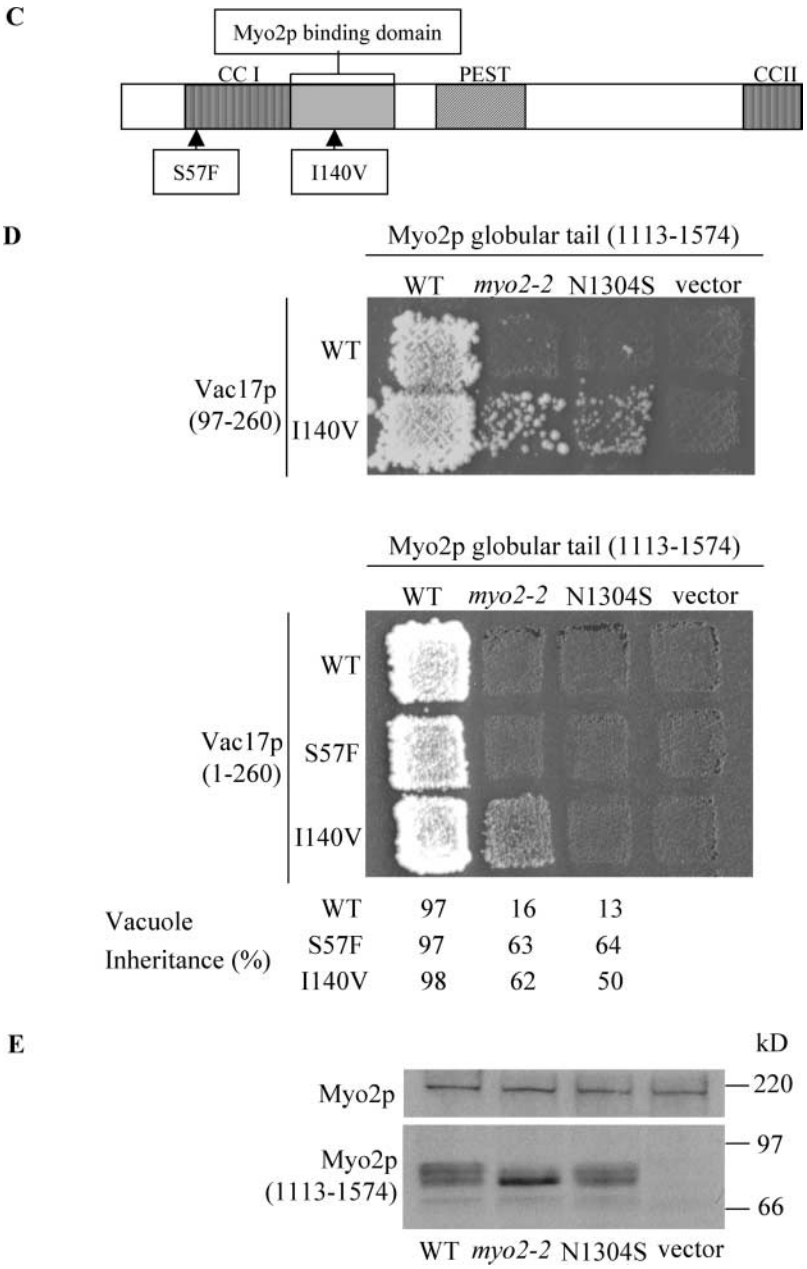

used to test I140V (residues 97–260) does not contain S57. Therefore, for direct comparison, the S57F and I140V mutations were each introduced into *VAC17* encoding 1–260. (E) Western blot analysis of the expression of the GAL4 binding domain-Myo2 globular tail fusion proteins (bottom) and endogenous Myo2p (top). The Western blot shown is representative of the results obtained in three independent experiments.

Alternatively, these myosin V receptors may each contain additional proteins. A portion of the vacuole-specific region of Myo2p (residues 1291–1313) is weakly conserved with all vertebrate myosins and is highly conserved among the three classes of vertebrate myosin Vs (Catlett et al., 2000; unpublished data). This suggests that this region in vertebrate myosin Vs may bind a protein receptor. Melanophilin, which binds to the melanocyte-specific exon F that is outside of the globular tail domain, may also bind to this conserved region; alternatively there may be yet another protein that binds this region and functions together with melanophilin and Rab27a. Notably, both the globular tail domain plus exon F are needed to observe the dominant-negative effects caused by overproduction of the myosin Va tail (Wu et al., 2002b).

Similarly, the vacuole-specific receptor reported here may also include a specific rab protein. Rab27a has been shown to be required for myosin Va binding to melanosomes, and Rab11a is required for myosin Vb binding to recycling endosomes (Lapierre et al., 2001). Moreover, the rabs, Sec4p (Schott et al., 1999; Ortiz et al., 2002), and Ypt31/Ypt32 (Ortiz et al., 2002) may play a role in Myo2p movement of secretory vesicles.

The discovery of organelle-specific myosin V receptors demonstrates that myosin V attaches to membranes via protein–protein interactions. Moreover, that Vac17p is not required for movement of other Myo2p cargo shows that within a single cell type, there are specific receptors for distinct membrane cargo. Perhaps these organelle-specific receptors compete with each other for access to the myosin V tail. Further study of Vac17p–Myo2p interactions will help elucidate how organelle-specific receptors regulate myosin V attachment to its diverse cargoes.

Materials and methods

The strains used in this paper are listed in Table II.

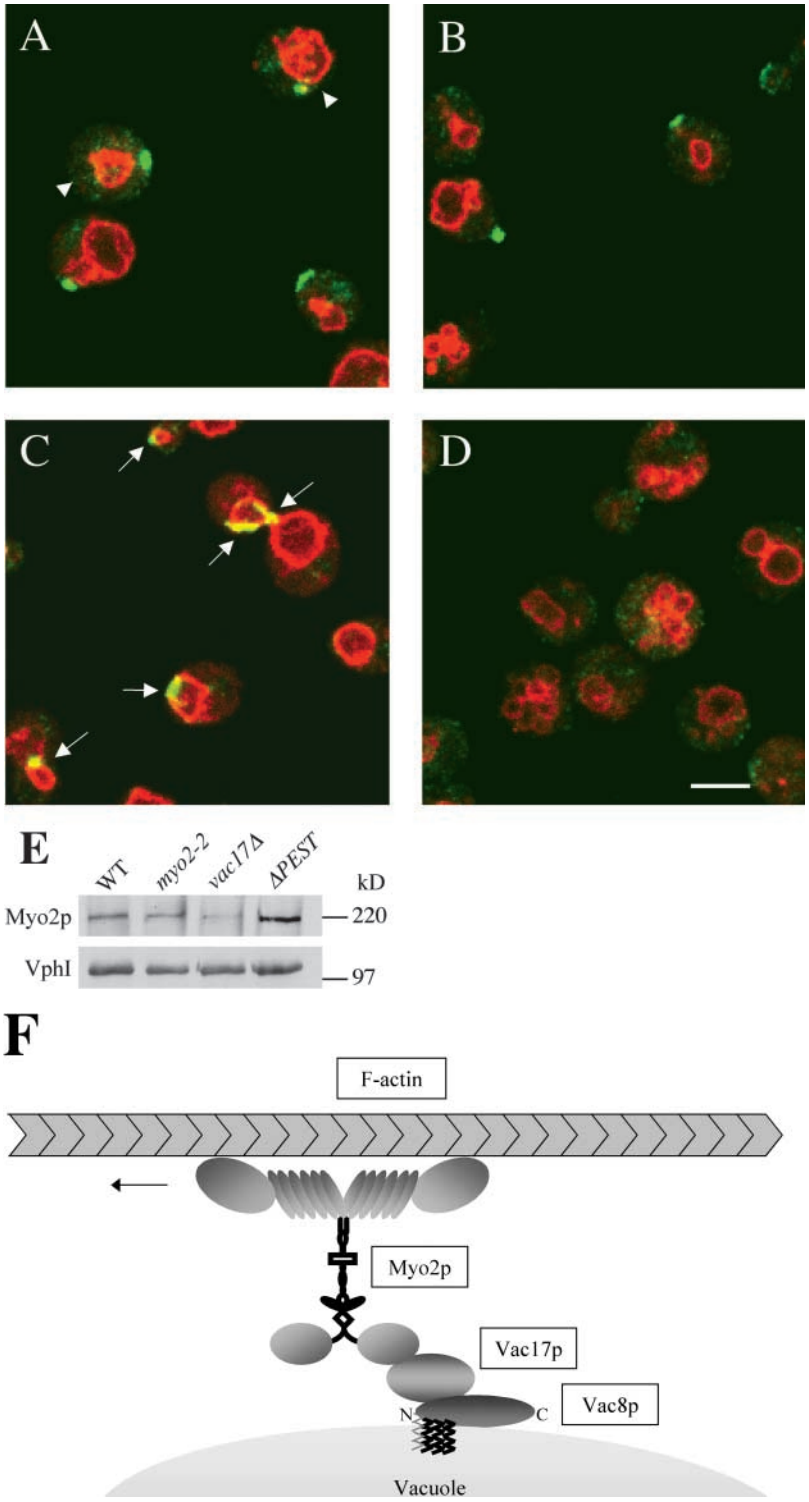

Figure 5. **Elevation of Vac17p levels on the vacuole membrane causes a corresponding increase of Myo2p on the vacuole membrane.** (A–D) Indirect immunofluorescence of Myo2p (green) and the 60-kD subunit of the yeast vacuolar ATPase (red). (A) Wild-type; LWY6726, pVAC17 (low copy plasmid). (B) *vac17*Δ; LWY6726, pRS416 (vector control). (C) *VAC17-*Δ*PEST*; LWY6726, p*VAC17-*Δ*PEST* (low copy plasmid). (D) *myo2–2*, LWY5518. Bar, 5 μm. Arrowheads indicate the low levels of Myo2p on the vacuole seen in wild-type cells (small yellow spots), whereas arrows indicate the increased levels of Myo2p on the vacuole seen in the *VAC17-*Δ*PEST* mutant cells. Vacuole inheritance is delayed in DBY1398 and the related strain LWY6726. Thus, the vacuole is not always juxtaposed with the site of bud emergence or the tips of small-budded cells and the sites of Myo2p accumulation on the vacuole membrane are not always coincident with these sites. These strains facilitate distinguishing between enrichment of Myo2p on the vacuole membrane versus enrichment at sites of polarized growth. (E) Western blot analysis of the levels of Myo2p (top) and yeast vacuolar ATPase 100-kD subunit (bottom) found on isolated vacuoles. A vector control (pRS416) was present in the first three strains. WT*, LWY7235; myo2–2, LWY5516; vac17*Δ, LWY5798; *VAC17-*Δ*PEST*, LWY5798, p*VAC17-*Δ*PEST* (low copy plasmid). The Western blot is representative of the results obtained in three independent experiments. (F) Model for Myo2p association with the vacuole. Vac17p binds directly to a vacuole-specific region of the globular tail domain of Myo2p. Vac17p interacts with the vacuole membrane via interaction with Vac8p. See Tang et al. (2003) for a detailed analysis of Vac17p association with Vac8p.

Plate assay for vacuole inheritance

The plate assay for vacuole inheritance (Gomes de Mesquita et al., 1996; Catlett et al., 2000) measures the maintenance of active carboxypeptidase Y (CPY), a vacuolar protease, after the inactivation of *PEP4*. *PEP4* encodes the first enzyme in the vacuolar protease cascade required for CPY activation. Strains were cotransformed with *pGAL-PEP4* and the indicated libraries, plasmids, or vector controls. Transformants were replica-plated to selective media containing 3% galactose, transferred to media containing 2% glucose, and then assayed for CPY activity. Wild-type colonies (VAC+) have active CPY and are red, whereas vacuole inheritance defective colonies (vac−) have inactive CPY and are white.

Screen for multicopy plasmids suppressing the *myo2–2* vacuole inheritance defect

Multicopy library pools RB378 and RB380, derived from YEp24 (*URA3*, 2μ), and the pRS202-based library (*URA3*, 2μ) were gifts from Drs. David Botstein (Stanford University, Stanford, CA) and Philip Hieter (University of British Columbia, Vancouver, BC), respectively. pNLC16 (p*GAL-PEP4-HIS3*) was generated by subcloning the EcoRI/SalI fragment from a URA-based *pGAL-PEP4* plasmid (Vida et al., 1990) into pRS413 (*HIS3*, CEN). LWY5518 yeast were cotransformed with pNLC16 and library DNA. Approximately 13,000, 45,000, and 19,000 transformants were screened from the pRS202 library and the RB378 and RB380 pools, respectively.

Table II. **Strains used in this paper**

Strain	Genotype	Source
LWY7235	*MATa, ura3-52, leu2-3,112, his3-Δ200, trp1-Δ901, lys2-801, suc2-Δ9*	Bonangelino et al., 1997
LWY5798	*MATa, ura3-52, leu2-3,112, his3-Δ200, trp1-Δ901, lys2-801, suc2-Δ9, vac17Δ::TRP1*	Tang et al., 2003
DBY1398	*MATa, ura3-52, ade2-1*	Thomas and Botstein, 1986
LWY6726	*MATa, ura3-52, ade2-1, vac17Δ:kanMX4*	This work; parental strain DBY1398
JP7A	*MATa, ura3-52, leu2-3,112, his6, met6, ade1, myo2-66*	Johnston et al., 1991
LWY5518	*MATa, ura3-52, leu2-3,112, his3-Δ200, trp1-Δ901, lys2-801, suc2-Δ9, pep4-Δ1137, myo2-2*	Catlett et al., 2000
LWY5516	*MATa, ura3-52, leu2-3,112, his3-Δ200, trp1-Δ901, lys2-801, suc2-Δ9, myo2-2*	This paper
LWY2949	*MATa, ura3-52, leu2-3,112, his3-Δ200, trp1-Δ901, lys2-801, suc2-Δ9, pep4-Δ1137, myo2Δ::TRP1, pMYO2*	Catlett et al., 2000
LWY2947	*MATa, ura3-52, leu2-3,112, his3-D200, trp1-Δ901, lys2-801, suc2-Δ9, myo2Δ::TRP1, pMYO2*	Catlett and Weisman, 1998
LWY6631	*MATa, ura3-52, leu2-3,112, his3-Δ200, trp1-Δ901, lys2-801, suc2-Δ9, pep4-Δ1137, myo2Δ::TRP1, vac17Δ::TRP1, pmyo2-N1304S-HIS3*	This work
PJ69-4A	*MATa, ura3-52, leu2-3,112, his3-200, trp1-901, gal4Δ, gal80Δ, LYS2::GAL1-HIS3, GAL2-AΔE2, met::GAL7-lacZ*	James et al., 1996
LWY6917	*MATa, ura3-52::GFP-PTS1-URA3, leu2-3,112, his3-Δ200, trp1-Δ901, lys2-801, suc2-Δ9*	Modified from Hoepfner et al., 2001
LWY6919	*MATa, ura3-52::GFP-PTS1-URA3, leu2-3,112, his3-Δ200, trp1-Δ901, lys2-801, suc2-Δ9, vac17Δ::TRP1*	Modified from Hoepfner et al., 2001
LWY6921	*MATa, ura3-52::GFP-PTS1-URA3, leu2-3,112, his6, met6, ade1, myo2-66*	Modified from Hoepfner et al., 2001
LWY6923	*MATa, ura3-52, leu2-3,112, his3-Δ200, trp1-Δ901, lys2-801, suc2-Δ9, SEC7Δ::SEC7-GFPx3*	Modified from Rossanese et al., 2001
LWY6927	*MATa, ura3-52, leu2-3, 112, his3-Δ200, trp1-Δ901, lys2-801, suc2-Δ9, vac17Δ::TRP1, SEC7Δ::SEC7-GFPx3*	Modified from Rossanese et al., 2001
LWY6931	*MATa, ura3-52, leu2-3,112, his6, met6, ade1, myo2-66, SEC7Δ::SEC7-GFPx3*	Modified from Rossanese et al., 2001
JSY3094	*MATa, ura3-52, his3Δ200, leu2Δ1, mdm20Δ::LEU2*	Singer et al., 2000

Vacuole inheritance was assessed with the CPY plate assay. As expected, *PEP4* was obtained; we also obtained *MYO2*. In addition, three isolates were obtained that restored vacuole inheritance to ~30% when assessed by fluorescence microscopy. Each contained a plasmid with multiple ORFs including full-length *VAC17* (YCL063W). *VAC17* was identified as the corresponding wild-type gene for the *vac* mutant *vac17–1*, and *VAC17* is required for vacuole inheritance (Tang et al., 2003). Thus, a multicopy plasmid containing *VAC17* alone was tested, and suppressed the vacuolar inheritance of *myo2–2* to a similar degree as the three candidate plasmids.

Screen for extragenic suppressors of the *myo2-N1304S* vacuole inheritance defect

myo2Δ::TRP1 yeast carrying plasmids *pmyo2-N1304S* and *pGAL-PEP4-URA3* were mutagenized with ethyl methanesulfonate as described previously (Winston, 1990). Vacuole inheritance was assessed with the CPY plate assay. VAC+ suppressor candidates were isolated, and the original *pmyo2-N1304S* plasmid was replaced with unmutagenized *pmyo2-N1304S* to distinguish between suppression due to a new mutation in the original *myo2-N1304S* plasmid or a mutation in another gene. One extragenic suppressor was identified out of 110,000 colonies. A heterozygous diploid of the suppressor candidate strain, with *myo2-N1304S* as the sole copy of *MYO2*, exhibited the same correction of vacuole inheritance as the haploid candidate strain, demonstrating that the suppressor mutation was dominant. In tetrads derived from this diploid, the restoration of vacuole inheritance segregated 2:2, indicating that the suppression arose from a single mutation. Therefore, a genomic library of this suppressor was constructed (see following paragraph) and transformed into the *myo2-N1304S* starting strain. Complementing plasmids were recovered and sequenced. The suppressing plasmid encoded *VAC17* with a single point mutation (C170T), resulting in the amino acid substitution S57F.

Construction of the genomic suppressor library

myo2-N1304S was integrated into the genome of the suppressor strain (*myo2Δ::TRP1, pMYO2-URA3*) via transformation and homologous recombination of a linear 5-kb fragment containing full-length *myo2-N1304S* (obtained from *pmyo2-N1304S* cut with ClaI, DraIII, and ScaI). The integrant was selected by growth on 5-fluoro-orotic acid plates and inability to grow on SC-TRP-URA plates. Size-fractionated (8–12 kb) genomic DNA from a partial Sau3A digest (techniques described in Nau et al., 1997) was ligated into the BamHI site of pRS415. Approximately 85% of the clones contained inserts.

Yeast two-hybrid analysis

Fusion of the GAL4 activation domain with *VAC17* (pGAD-*VAC17*) is described in Tang et al. (2003). For pRS416-*VAC17*(1–170), pRS416-*VAC17* was cut with BstBI and religated, creating K171N, T172L, and N173-STOP. For pGAD-*VAC17*(1–170), an ~1.2-kb BglII and PacI fragment from pGAD-*VAC17* was replaced with the corresponding fragment from pRS416-*VAC17*(1–170). For pGAD-VAC17(97–170), the ~500-bp EcoRI fragment from pRS416-*VAC17*(1–170) was cloned into the EcoRI site of pGAD-C1 (James et al., 1996). For pRS416-*VAC17*(1–355), pRS416-*VAC17* was cut with AflII, the sticky ends were filled in with Klenow, and the plasmid was religated, creating K356-STOP. For pGAD-*VAC17*(1–355), the BglII and PacI fragment from pGAD-*VAC17* was replaced with the corresponding fragment from pRS416-*VAC17*(1–355). For the pGAD-VAC*17*(97–260) plasmids, DNA was amplified from either pRS416-*VAC17*, pRS416-*vac17-S57F*, or pRS415-*vac17-I140V* using primers TF1v (5′-AAAAGGATCCATGGCAACCCAAGCCCTAGAG-3′) and VAC17 Cla3R (5′-GGATCGATTTCAGCACCCTTTGCGGGCACACC-3′), which add BamHI and ClaI sites, respectively, and was ligated into pGAD-C1.

For the pGBD-*MYO2*(1113–1574) clones, DNA for all mutants and wild-type were PCR amplified from the relevant *MYO2* plasmids (Catlett et al., 2000) using the MYO2-Bam3F (Catlett et al., 2000) and T3 universal primers. PCR products were cut with BamHI and ClaI and ligated into pGBD-C1 (James et al., 1996). To generate pGBD-*myo2 1113–1574 Δ1459–1491*, the ~1.5-kb BamHI and ClaI fragment of pNLC27 (Catlett, 2000) was subcloned into pGBD-C1.

The following *MYO2* deletions were generated with the QuikChange® Site-Directed Mutagenesis Kit (Stratagene) using a pBluescript plasmid (NLC15) containing the 1.6-kb EcoRI fragment of pRS413-*MYO2* (Catlett and Weisman, 1998). For pGBD-C1-*myo2 1113–1518*, the primers SDP 7F (5′-GGGTCACGAGCATAGCTGAAGCATATTTATCACTCC-3′) and SDP 7R (5′-GGAGTGATAAATATGCTTCAGCTATGCTCGTGACCC-3′) were used to generate a stop codon at amino acid 1518. For pGBD-C1-*myo2 1113–1574 Δ1297–1307*, the primers SDP 9F (5′-GGTCACAGAAC-TAAAGGATATTTGGCTGAAGAAATTGCAG-3′) and SDP 9R (5′-CTG-CAATTTCTTCAGCCAAATATCCTTTAGTTCTGTGACC-3′) were used. The ~1.3-kb StuI and ClaI fragments from the above plasmids were each li-

gated into pGBD-*MYO2 1113–1574* missing the corresponding region. For pGBD-*myo2 1113–1568*, the primers SDP 8F (5′-GACCTTGTTGCCCAATAAGTCGTTCAAGACGG-3′) and SDP 8R (5′-CCGTCTTGAACGACTTATTGGGCAACAAGGTC-3′) were used to generate a stop codon at amino acid 1568. The ~1.5-kb EcoRI and ClaI fragment was subcloned into pGBD-C1-*myo2 1113–1574* missing the corresponding region.

Random mutagenesis of *VAC17*

To isolate *VAC17* suppressors of *myo2-N1304S*, PCR mutagenesis was performed using Taq DNA polymerase (Boehringer). Full-length *VAC17* was PCR amplified from *pRS415-VAC17* using the primer set TF1v (see above) and TF2v (5′-AAAACTGCAGAAGATGGCACCCGAGTCTAG-3′). LWY6631 (*pGAL-PEP4 -URA*) was cotransformed with the mutated *VAC17* PCR products and a *VAC17* plasmid cut with MscI and SphI to remove most of *VAC17*.

In vivo labeling of organelles

Yeast vacuoles were labeled with N-(3-triethylammoniumpropyl)-4(6(4(diethylamino)phenyl)hexatrienyl) pyridium dibromide (FM4–64; Molecular Probes, Inc.) as described previously (Catlett et al., 2000). Low and high copy *VAC17* were expressed from the pRS416 and pRS426 plasmids, respectively (Tang et al., 2003). Nuclei were observed with 4′ DAPI dihydrochloride hydrate (Sigma-Aldrich) as described previously (Sherman et al., 1986).

Immunofluorescence labeling and vacuole purification

Indirect immunofluorescence was performed essentially as described previously (Hill et al., 1996; Catlett et al., 2000). Goat anti-Myo2p tail antiserum (Catlett, 2000) was affinity purified as previously described (Reck-Peterson et al., 1999). Fixed cells were incubated with affinity-purified goat anti-Myo2p tail antibody (1:200), followed by Alexa 488-donkey anti–goat IgG (1:200). Vacuole membranes were labeled with mouse anti–yeast v-ATPase 60-kD subunit (1:200), followed by Rhodamine red X-donkey anti–mouse IgG (1:200). Secondary antibodies and anti–yeast v-ATPase were purchased from Molecular Probes, Inc.

Vacuoles were isolated on a Ficoll flotation gradient as described previously (Catlett and Weisman, 1998), except 40 μM chymostatin, 10 mM DTT, 1× complete, EDTA-free protease inhibitor cocktail (Roche), and 1× protease inhibitor cocktail (Sigma-Aldrich), were added to the cell suspension and Ficoll gradient layers. After removal from the gradient, vacuoles were washed once in the gradient buffer and collected by centrifugation at 13,000 *g* for 10 min.

Fluorescence microscopy

Cells were viewed with a microscope (Axioscope 2, Carl Zeiss MicroImaging, Inc.) equipped for epifluorescence, and images were captured using an RT Spot camera (Diagnostic Instruments, Inc.) controlled by MetaMorph® Imaging Series 4.5 software (Universal Imaging Corporation).

Confocal images were obtained with a laser scanning confocal microscope (model LSM 510; Carl Zeiss MicroImaging, Inc.). For each field, a z-series of 0.3-μm slices was scanned and projected to generate a single image. The data was exported as 8-bit TIFF files and processed using Adobe Photoshop®.

Western blot analysis

SDS-PAGE and Western blot analysis were performed after standard procedures. Primary and secondary antibodies were used at the following concentrations: affinity-purified goat anti-Myo2p tail (1:2,000), HRP-donkey anti–goat IgG (1:5,000; Jackson ImmunoResearch Laboratories), mouse anti–yeast v-H^+-ATPase 100-kD subunit (1:5,000; Molecular Probes, Inc.), and HRP-goat anti–mouse IgG (1:5,000; Molecular Probes, Inc.). For Fig. 3 E, the concentrations of primary and secondary antibodies were goat anti-Myo2p tail (1:10,000) and HRP-donkey anti–goat IgG (1:10,000). HRP activity was detected using ECL (Amersham Biosciences).

We thank Dr. Henk Tabak (University of Amsterdam, Amsterdam, Netherlands), for communicating results before publication. We thank Yutian Peng for construction of the yeast strain LWY6631. We thank Drs. Tabak, Benjamin Glick (University of Chicago, Chicago, IL), and Janet Shaw (University of Utah, Salt Lake City, UT) for strains and plasmids. We thank Drs. David Botstein and Philip Hieter for the multicopy libraries. We thank Tom Monninger and Randy Nessler and the University of Iowa Central Microscopy Research Facility for guidance in the use of the confocal microscope. We thank Drs. Robert Cohen, John Donelson, Robert Piper, Peter Rubenstein, and Mark Stamnes for helpful discussions.

This work was supported by the National Institutes of Health (grant RO1 GM62261), the National Science Foundation (MCB 96-00867), and an Established Investigator Award from the American Heart Association (0140233N; to L.S. Weisman). N.L. Catlett was supported in part by a National Institute on Aging Grant (T32 AG 00214) awarded to The Interdisciplinary Research Training Program on Aging, University of Iowa.

Submitted: 24 October 2002
Revised: 17 January 2003
Accepted: 23 January 2003

References

Beach, D.L., J. Thibodeaux, P. Maddox, E. Yeh, and K. Bloom. 2000. The role of the proteins Kar9 and Myo2 in orienting the mitotic spindle of budding yeast. *Curr. Biol.* 10:1497–1506.

Bonangelino, C.J., N.L. Catlett, and L.S. Weisman. 1997. Vac7p, a novel vacuolar protein, is required for normal vacuole inheritance and morphology. *Mol. Cell Biol.* 17:6847–6858.

Catlett, N.L. 2000. Role of a yeast myosin-V in movement of the vacuole and other cargoes. *In* Department of Biochemistry. University of Iowa, Iowa City. 135.

Catlett, N.L., and L.S. Weisman. 1998. The terminal tail region of a yeast myosin-V mediates its attachment to vacuole membranes and sites of polarized growth. *Proc. Natl. Acad. Sci. USA.* 95:14799–14804.

Catlett, N.L., J.E. Duex, F. Tang, and L.S. Weisman. 2000. Two distinct regions in a yeast myosin-V tail domain are required for the movement of different cargoes. *J. Cell Biol.* 150:513–526.

Fukuda, M., and T.S. Kuroda. 2002. Slac2-c (synaptotagmin-like protein homologue lacking C2 domains-c), a novel linker protein that interacts with Rab27, myosin Va/VIIa, and actin. *J. Biol. Chem.* 277:43096–43103.

Gomes de Mesquita, D.S., H.B. van den Hazel, J. Bouwman, and C.L. Woldringh. 1996. Characterization of new vacuolar segregation mutants, isolated by screening for loss of proteinase B self-activation. *Eur. J. Cell Biol.* 71:237–247.

Govindan, B., R. Bowser, and P. Novick. 1995. The role of Myo2, a yeast class V myosin, in vesicular transport. *J. Cell Biol.* 128:1055–1068.

Hill, K.L., N.L. Catlett, and L.S. Weisman. 1996. Actin and myosin function in directed vacuole movement during cell division in *Saccharomyces cerevisiae*. *J. Cell Biol.* 135:1535–1549.

Hoepfner, D., M. van den Berg, P. Philippsen, H.F. Tabak, and E.H. Hettema. 2001. A role for Vps1p, actin, and the Myo2p motor in peroxisome abundance and inheritance in *Saccharomyces cerevisiae*. *J. Cell Biol.* 155:979–990.

Hume, A.N., L.M. Collinson, C.R. Hopkins, M. Strom, D.C. Barral, G. Bossi, G.M. Griffiths, and M.C. Seabra. 2002. The leaden gene product is required with Rab27a to recruit myosin Va to melanosomes in melanocytes. *Traffic.* 3:193–202.

James, P., J. Halladay, and E.A. Craig. 1996. Genomic libraries and a host strain designed for highly efficient two-hybrid selection in yeast. *Genetics.* 144: 1425–1436.

Johnston, G.C., J.A. Prendergast, and R.A. Singer. 1991. The *Saccharomyces cerevisiae* MYO2 gene encodes an essential myosin for vectorial transport of vesicles. *J. Cell Biol.* 113:539–551.

Karcher, R.L., J.T. Roland, F. Zappacosta, M.J. Huddleston, R.S. Annan, S.A. Carr, and V.I. Gelfand. 2001. Cell cycle regulation of myosin-V by calcium/calmodulin-dependent protein kinase II. *Science.* 293:1317–1320.

Lapierre, L.A., R. Kumar, C.M. Hales, J. Navarre, S.G. Bhartur, J.O. Burnette, D.W. Provance, Jr., J.A. Mercer, M. Bahler, and J.R. Goldenring. 2001. Myosin vb is associated with plasma membrane recycling systems. *Mol. Biol. Cell.* 12:1843–1857.

Melkonian, K.A., A.G. Ostermeyer, J.Z. Chen, M.G. Roth, and D.A. Brown. 1999. Role of lipid modifications in targeting proteins to detergent-resistant membrane rafts. Many raft proteins are acylated, while few are prenylated. *J. Biol. Chem.* 274:3910–3917.

Nagashima, K., S. Torii, Z. Yi, M. Igarashi, K. Okamoto, T. Takeuchi, and T. Izumi. 2002. Melanophilin directly links Rab27a and myosin Va through its distinct coiled-coil regions. *FEBS Lett.* 517:233–238.

Nau, J.J., K.R. Summers, A.M. Galbraith, S.A. Bullard, and R.E. Malone. 1997. Isolation of early meiotic recombination genes analogous to *S. cerevisiae* REC104 from the yeasts *S. paradoxus* and *S. pastorianus*. *Curr. Genet.* 31:7–14.

Ortiz, D., M. Medkova, C. Walch-Solimena, and P. Novick. 2002. Ypt32 recruits the Sec4p guanine nucleotide exchange factor, Sec2p, to secretory vesicles; evidence for a Rab cascade in yeast. *J. Cell Biol.* 157:1005–1015.

Provance, D.W., T.L. James, and J.A. Mercer. 2002. Melanophilin, the product of the leaden locus, is required for targeting of myosin-Va to melanosomes. *Traffic*. 3:124–132.

Reck-Peterson, S.L., P.J. Novick, and M.S. Mooseker. 1999. The tail of a yeast class V myosin, Myo2p, functions as a localization domain. *Mol. Biol. Cell.* 10:1001–1017.

Rossanese, O.W., C.A. Reinke, B.J. Bevis, A.T. Hammond, I.B. Sears, J. O'Connor, and B.S. Glick. 2001. A role for actin, Cdc1p, and Myo2p in the inheritance of late Golgi elements in *Saccharomyces cerevisiae*. *J. Cell Biol.* 153:47–62.

Schott, D., J. Ho, D. Pruyne, and A. Bretscher. 1999. The COOH-terminal domain of Myo2p, a yeast myosin V, has a direct role in secretory vesicle targeting. *J. Cell Biol.* 147:791–808.

Sherman, F., G.R. Fink, and J.B. Hicks. 1986. Methods in Yeast Genetics. Cold Spring Harbor Laboratory Press, Cold Spring Harbor, NY. 153 pp.

Singer, J.M., G.J. Hermann, and J.M. Shaw. 2000. Suppressors of mdm20 in yeast identify new alleles of ACT1 and TPM1 predicted to enhance actin-tropomyosin interactions. *Genetics.* 156:523–534.

Tang, F., E.J. Kauffman, J.L. Novak, J.J. Nau, N.L. Catlett, and L.S. Weisman. 2003. Regulated degradation of a class V myosin receptor directs movement of the yeast vacuole. *Nature*. 10.1038/nature01453.

Thomas, J.H., and D. Botstein. 1986. A gene required for the separation of chromosomes on the spindle apparatus in yeast. *Cell.* 44:65–76.

Vida, T.A., T.R. Graham, and S.D. Emr. 1990. In vitro reconstitution of intercompartmental protein transport to the yeast vacuole. *J. Cell Biol.* 111: 2871–2884.

Wang, Y.X., E.J. Kauffman, J.E. Duex, and L.S. Weisman. 2001. Fusion of docked membranes requires the armadillo repeat protein Vac8p. *J. Biol. Chem.* 276: 35133–35140.

Winston, F. 1990. Mutagenesis of yeast cell. *In* Current Protocols in Molecular Biology. F.M. Ausubel, R. Brent, R.E. Kingston, D.D. Moore, J.A. Smith, J.G. Seidman, and K. Struhl, editors. Greene Publishing Associates and Wiley-Interscience, New York. 13.3.1–13.3.4.

Wu, X., F. Wang, K. Rao, J.R. Sellers, and J.A. Hammer III. 2002a. Rab27a is an essential component of melanosome receptor for Myosin va. *Mol. Biol. Cell.* 13:1735–1749.

Wu, X.S., K. Rao, H. Zhang, F. Wang, J.R. Sellers, L.E. Matesic, N.G. Copeland, N.A. Jenkins, and J.A. Hammer III. 2002b. Identification of an organelle receptor for myosin-Va. *Nat. Cell Biol.* 4:271–278.

Yin, H., D. Pruyne, T.C. Huffaker, and A. Bretscher. 2000. Myosin V orientates the mitotic spindle in yeast. *Nature.* 406:1013–1015.

Zacharias, D.A., J.D. Violin, A.C. Newton, and R.Y. Tsien. 2002. Partitioning of lipid-modified monomeric GFPs into membrane microdomains of live cells. *Science.* 296:913–916.